The influence of wind turbines on dualpol radar moments and products

Michael Frech*and Jörg Seltmann, Deutscher Wetterdienst
Hohenpeissenberg Meteorological Observatory, Germany

October 2, 2017

1. Introduction

There is a strong political and economic push to further expand renewable energy production in order to reduce the dependence on for example coal burning power plant and to achieve the CO_2 reduction goals. The contribution of renewable energy production relies mainly on solar energy and wind power. The preferred location for wind turbines are areas with sufficient wind potential, such as off-shore areas, plains or mountain ranges. The increasing number of installed wind turbines is causing concern among weather radar operators and users. Basically, this is due to the difficulties to filter out the contribution of a wind turbine in the radar return signal from the weather return signal. Here, classic Doppler clutter filters do not work properly because of the moving rotor blades. So far new filter methods have not been developed for operational usage which could reliably remove the wind turbine signal and recover the weather signal. There are proposals to simply replace and fill the wind turbines contaminated area with radar information from undisturbed neighboring areas. This may be a possible approach for singular wind mills, but not for wind farms which often cover a much larger area.. Radar operators try to keep a wind turbine free zone around radars. A WMO recommendation proposes a 20 km area around a wind turbine to avoid the negative impact. However, this limit often cannot be guaranteed because radar locations are also preferred areas for wind turbines so that there is a strong pressure to accept wind mills in closer vicinity of a weather radar. The concern of weather services is, that they are no longer able to provide reliable warnings of adverse weather to the public because of corrupted radar data. Warnings with a lead time of about 30 minutes are typically based on automated algorithms which primarily rely on observational data. Radar data are key here as it is the only instrument which can provide spatial and volumetric information of the atmospheric state at high spatial and temporal resolution. The skill of forecast models at this time scale is not sufficient. Severe weather warnings often associated with large radar reflectivity factors (e.g. hail) may be significantly compromised by the signal of wind turbines.

A complicating effect is that the influence of wind turbines is not confined to its physical location. A much larger volume can be affected due to the transmission and reception of energy through the antenna side lobe or multi-path effects (Norin, 2014).

There are only a few studies on the influence of wind farms on DualPol data (Frech and Seltmann, 2014, Keranen et al., 2014). In this contribution we summarize the work presented in (Frech and Seltmann, 2014) and further extend the analysis on influences on radar data based products. To this end we have implemented dedicated "clutter target scans", where we dwell at a target for some time with the antenna put on hold. These scans are repeated every 5 minutes as part of DWD's operational scan strategy. This allows us to acquire sufficient samples to investigate the effect of a wind turbine in a statistical way. Here we investigate data from the radar Prötzel (PRO) where we have setup a scan to monitor a number

*Corresponding author address: Michael Frech, DWD, Meteorologisches Observatorium Hohenpeissenberg, D-82383 Hohenpeissenberg, Germany. Email: Michael.Frech@dwd.de
Poster 271, extended abstract, AMS Radar conference 2017, Chicago, Il, USA.

of wind turbines just 15 km away from the radar which are compared to data from a additional clutter target scan pointing to TV tower. Latter target can be considered as a typical clutter target.

2. The DWD radar network

The German Meteorological Service DWD is operating the national radar network. The network consists of 17 C-Band radar systems which cover the German territory. An additional system serves as a research radar which is operated at the Hohenpeissenberg Observatory. There, new technologies, radar data processing algorithms, radar software and data quality monitoring tools are developed, tested and evaluated before they are introduced into operational service. All but one radar are EEC's Doppler weather radar DWSR5001C/SDP/CE with polarization diversity (SDP, simultaneous dual polarization).

Here we summarize briefly some key aspects of the radar system and its setup:

Pedestal unit: pointing accuracy $< 0.05°$, maximum azimuth rate 48 °/s

Transmitter: Magnetron based transmitter, peak power 500 kW (so 250 kW for the H and V channel each). Frequency range 5600 to 5650 MHz. Four pulse widths: 0.4, 0.6, 0.8 and 2 μs.

Receiver: The receiver is mounted behind the antenna ("receiver-over-elevation" concept). The analog signals are digitized by the ENIGMA3p IFD and the digitized IQ-data are transmitted in realtime through a fiber optic rotary joint to the ENIGMA3p signal processor which is mounted in the radar control cabinet. The dynamic range of the dual IF receiver is $\geq$ 105 dB.

Signal processor: GAMIC's Linux based signal-processor ENIGMA3p

Antenna: The parabolic antenna has a diameter of 4.3 m and consists of 9 elements. The dish is made of a composite material and has a center-fed antenna design with four struts supporting the dualpol feed.

Radome: AFC radome 20DSF17 with a quasi random panel design optimized for dualpol applications. The panels have a sandwich foam core design. The radome is coated with a highly hydrophobic material and has a diameter of 6 m.

In the operational scanning we use two pulse widths, 0.4 and 0.8 μs.

3. Clutter target scans and data analysis

Two dedicated clutter target scans are set up at the radar site Prötzel.

The classic clutter target scan points at a TV tower (CT) at range $r = 16.83$ km, at an elevation $el = 0.3°$, azimuth $az = 266.3°$. The wind turbine clutter target (WT) is at $r = 13.87$ km, $az = 69.2°$ and $el = 0.5°$. The hub height is around 125 m, rotor radius 45 m. Assuming a beam width of 1°, geometrically only sweeps at 0.5° are expected to be affected by the presence of a WT with the given dimensions. The scans are parameterized with a pulse width of 0.8 μs, PRF $= 1000$ Hz, time sampling of 128 pulses and and a dwell time of 2 seconds (this amounts to about 15 samples) The range sampling is set to 25 m. In addition, we extract the corresponding radar moments from range bins of the precipitation scan (orography following scan optimized for hydrological products) and the volume scan at elevations 0.5, 1.5 and 2.5°. The range bin resolution is 500 m for the precipitation scan and 1000 m for the volume scan. Clutter micro suppression (CMS) is activated. CMS works on the raw-rangebin (range sampling at 25 m) and is parameterized in terms of a clutter power threshold which is set to -30 dB. If the clutter power of the raw rangebin is smaller than this threshold, it is censored prior range averaging. Those data are extracted at the radar site prior the final POLARA quality control and product generation. In order to analyse the influence of clutter targets on final products, we also consider results of the hydrometeor classification (HMC) from WT range bin. The products are compared to data from a weather station (Manschnow, WMO id 10396) which is at a range of 47 km from the radar. This is not ideal but it is the closest site available for this WT site.

Figure 1: The clutter target Prötzel TV tower.

The classic clutter target is shown in Figure 1. The wind farm site map is shown in Figure 2.

4. DWD hydrometeor classification

The DWD dualpol hydrometeor classification algorithm Hymec is based on a fuzzy logic scheme (Frech and Steinert, 2015). The usage of a fuzzy logic method is well established (Park et al., 2009 and Al-Sakka et al., 2013). To feed the fuzzy logic scheme, trapezoidal membership functions (MBF) for each input parameter (namely the radar reflectivity factor Zh, the differential reflectivity ZDR, the cross correlation coefficient ρ_{hv}, the differential specific phase KDP, the height of the zero degree level HZEROCL, and the snow height level SNOWLMT) are created. Hymec considers the hydrometeor types drizzle, rain, big drops, melting particles (including the bright band), wet snow, dry snow, ice crystals, Graupel, heavy rain / hail and hail. The detection of the light rain class (drizzle) and a separate class for the melting layer is of particular high importance for forecasters because of regionally long lasting drizzle events that are common in

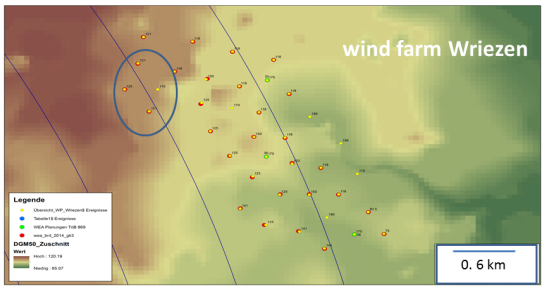

Figure 2: Map of the Wriezen wind farm. Circled in blue is area of which is illuminated with with WT scan.

Germany.

5. Time series of a clutter target (TV tower) and wind turbine

We first summarize some overall features of wind turbine signatures in radar data. Those observations are compared to features that are observed for a "pure" clutter target. The clutter powers as computed from the clutter target scan and the operational precipitation scan are shown in Figure 3. These plots are taken as a baseline against which filtered and unfiltered radar moments are analyzed. The data shown in Figures 3, 4 and 5 are from a precipitation event on 12.7.- 13.7.2017. The beginning of precipitation was around 11:00 UTC and lasted until about 22:00 UTC. The following observations can be made:

- Clutter power (ccorh and ccorv): The clutter power is near -50 dB for the clutter target. The clutter power of the WT shows significant variability. Clutter power up to -50 dB can be observed initially, but approaches values close to zero during the precipitation event. One explanation for this is that the WT behaves like a classic clutter target if the rotor blades do not move, or if the rotor blades are perpendicular to the wave front. The clutter power from the pre-

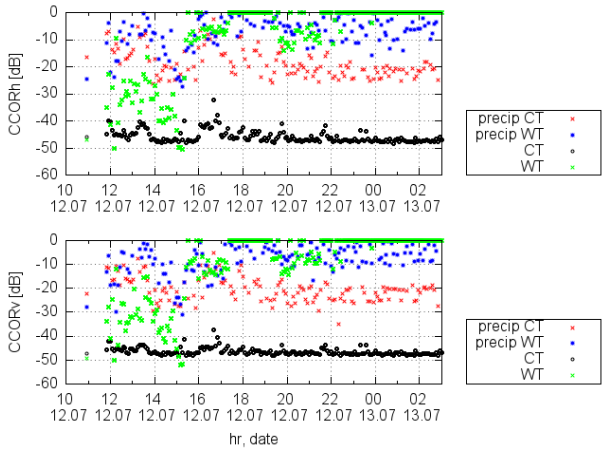

Figure 3: Computed clutter power based on the clutter target scans and the operational precipitation scan. CT denotes the clutter target (TV tower), WT denotes the clutter target wind turbine. "precip CT" represent data of the operational range bin containing the clutter target CT. Similarly "precip WT" are data from the WT range bin.

cipitation scan is significantly smaller. For the CT, we find about -20 dB or less, and -10 dB and smaller values for the WT. This can be related to fact, that the target is not ray filling (not all pulse are on target while the radar scans over the WT). For both targets (CT and WT), both the horizontal and vertical polarization show similar magnitude in clutter power.

- Zh: The Doppler clutter filter is most effective for the clutter target. The unfiltered Zh has a constant level of 70 dBZ for the CT, and about 50 dBZ for the WT. Applying the clutter filter, the CT signal is effectively filtered (no signal larger 0 dB). The clutter filter fails to remove the WT signal most of the time. The filtered Zh is still near 50 dBZ. Only in the beginning, when the WT target behaves as a classic clutter target, part of the clutter signal can be removed, where Zh is then on the order of 20 dBZ. For the data from the operational precipitation scan, the WT has approximately a constant level of 20 dBZ for both the unfiltered and Doppler filtered data. This is also seen after the end of the precipitation event. Clutter micro suppression CMS is used in the precip-

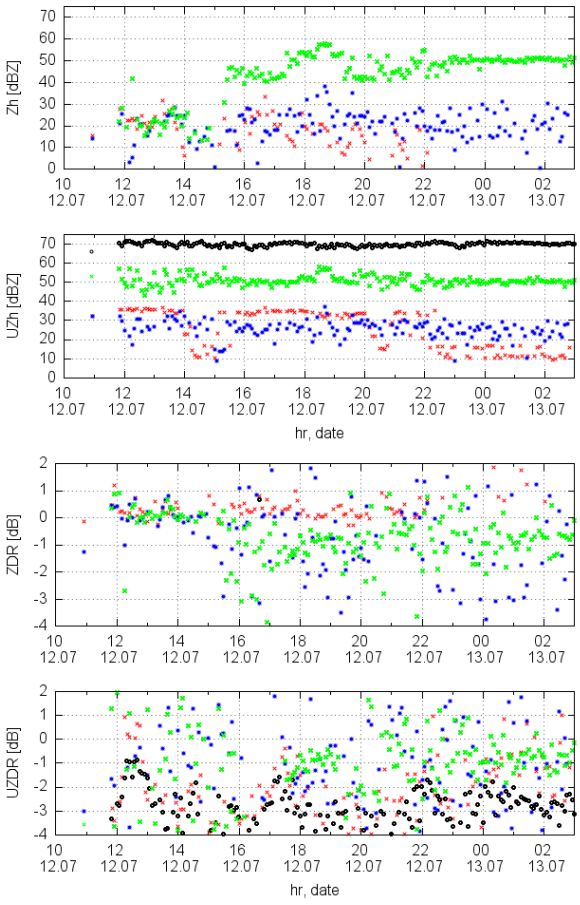

Figure 4: The corresponding Doppler filtered and unfiltered reflectivity factor Zh and UZh, respectively, and the Doppler filtered and unfiltered differential reflectivity ZDR and UZDR, respectively, for the clutter scans and the precipitation scans (see also 3). For the legend, see Figure 3.

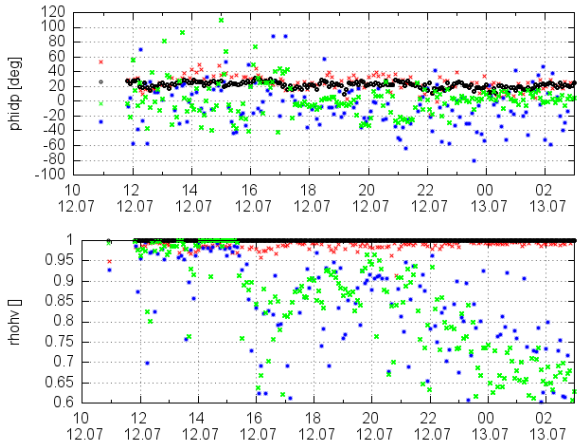

Figure 5: The corresponding Φ_{dp} and ρ_{hv} for the clutter and precipitation scans (see 3). For the legend, see Figure 3.

itation scan and presumably does not perform well because of the variable nature of the clutter power (temporally and spatially) and the influence of other WT in the vicinity. With CMS, the clutter power on the raw-range bin level (prior range averaging) is compared to a predefined clutter power threshold (currently set to 30 dB). If the clutter power exceeds this threshold, the range bin is discarded before the range averaging. Contrary to the WT data from the precipitation scan the CT signal more often can be separated from the weather signal through CMS.

- ZDR: Considering the unfiltered differential reflectivity, namely UZDR, we find considerable scatter for all 4 time series. However some characteristic features seem to emerge: the CT UZDR approximately is -2 dB and shows a variation of about $\pm$ 1 dB. In contrast, the WT values tend to be also negative on average but with a significantly larger scatter including a number of positive values. In principle this can also be observed with the UZDR data from the precipitation scan. There, the scatter appears larger which may be attributed to the involved range averaging and due to targets that are not ray filling. Applying the Dopper clutter filter, the CT UZDR is effectively filtered, which is consistent with what obtain for Zh. No precipitating signal is recovered. CT ZDR from the precipitation scan are now mainly positive (about 0.2 dB, which is typical for precipitation; recall that precipitation is observed here) which indicates that the static clutter has been removed successfully by the Doppler clutter filter. In contrast, for both WT time series the scatter in ZDR remains large and in particular the WT ZDR time series remains mostly negative, clearly indicating that the Doppler filter can remove the WT signal. Latter is also true for the ZDR from the precipitation scan.

- Φ_{dp}: First of all: operationally, we use unfiltered Φ_{dp} data in order to avoid biases from the Doppler clutter filter. The values are around 20° for the CT data (the hardware dependent $\Phi_{dp,0}$ is set to 20°) . There is large scatter for the WT data, with a tendency towards values below 0°. This is seen for the clutter scan and the operational scan. Φ_{dp} based algorithms and corrections are therefore expected to be biased due the presence of WT.

- ρ_{hv}: First of all: operationally, we use unfiltered ρ_{hv} data in order to avoid biases from the Doppler clutter filter. So we consider here only the unfiltered time series. The cross correlation coefficient is ≈ 1 for both the CT data and CT data from precipitation scan. Obviously, ρ_{hv} is dominated by the CT. This is true for both non-precipitating and precipitating situations. Both time series for the WT show much larger scatter and significantly larger deviations from 1 which are could be associated non-meteorological echoes.

6. Hydrometeor classification

In the previous section we have identified some distinct differences between classic clutter target and and WT target, in particular for the dualpol moments. The question arises how those differences impact products like the hydrometeor classification (HMC). This will be investigated in this section based on a precipitation event 12 July 2017. We compare the classification results of a radar range bin located over a wind farm with a range bin situated over a weather station. The time-height plot of HMC for the WT

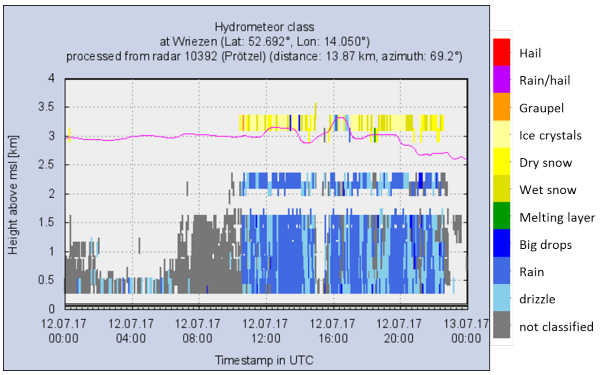

Figure 6: Time height plot of hydrometeor classification results on 12 July 2017, for a radar rangebin at the boundary of the Wriezen wind farm, see figure

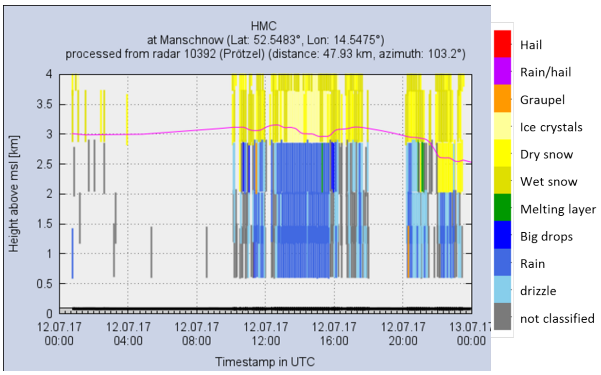

Figure 7: Time height plot of hydrometeor classification results on 12 July 2017, for a radar range bin over the Manschnow site, which serves as a reference.

case is shown in Figure 6 and the corresponding plot for the weather station in Figure 7.

The most striking difference is that the number of classified and non-classified range bins prior to the precipitation onset (around 10 UTC) is significant larger for the WT target (Figure 6) compared to the weather station site (Figure 7). This suggests, that there are data which pass the operational quality control. However the range of those data cannot be associated to a certain HM type in the fuzzy logic classifier. For this situation, they are assigned as being "not classified". It should be emphasized that even though there is no HM classification possible, the radar moments, which have passed the quality control, appear as valid measurements.

The correlation coefficient ρ_{hv}, differential reflectivity ZDR, radar reflectivity factors and the HM probability are shown in Figures 8, 9 and 10, respectively. Here we show only the radar moments for the Wriezen site. Prior to the onset of precipitation, small Zh levels ranging from -10 to +10 dBZ are present not just close to the surface but up to 1.5 km above the surface. Close to the surface (below 500 m) Zh values are commonly around 10 dBZ. Compared to the time period with precipitation, ZDR shows significantly larger scatter ranging from -2 to +4 dB. ρ_{hv} values range from 0.6 to 0.8 which is indicative of non-meteorological echoes. With this set of radar moments, the HMC classification identifies drizzle and rain over consecutive radar measurements, in particular at the lowest elevation where we find ZDR and ρ_{hv} values which can be associated with meteorological scatterer. The low Zh values between 6:00 and 10:00 UTC, which can be seen up to 1500 m may be viewed as indicative of biological scatterer trapped in the atmospheric boundary layer. However, our existing HMC scheme does not consider such a class. In contrast, if we consider the HM results at the Manschnow site, there are, as expected, significantly less HM classifications before the onset of precipitation. In this case, the quality control successfully separates meteorological and non-meteorological scatterer most of the time. This suggests that the large number of classified pixels at the Wriezen site prior to the onset of precipitation is due to the presence of WTs.

The Wriezen radar range bin that is investigated here is situated at the boundary of the wind farm (Figure 2). So previous analysis refers to radar measurements at the boundary of the Wriezen wind park. Within the area of the wind farm, radar data are thresholded by quality control so that no HM can be diagnosed (Figure 11). The operational quality control is based on a fuzzy logic classifier (Werner, 2013) where for example clutter power and the texture of Φ_{dp} is considered. Most likely the texture of Φ_{dp} leads to the thresholding of the wind farm area. Large texture values of Φ_{dp} can be expected if we consider the large variability of Φ_{dp} in Figure 5 for the WT data. From a data quality control point of view this is encouraging (we are able to identify data with questionable

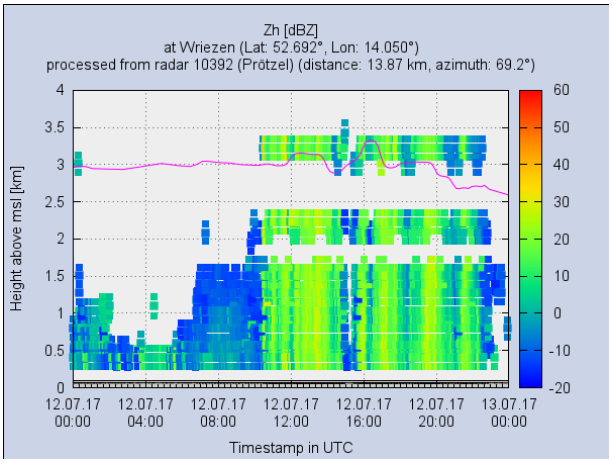

Figure 8: Time-height plot of Zh 12 July 2017 for the Wriezen reference bin

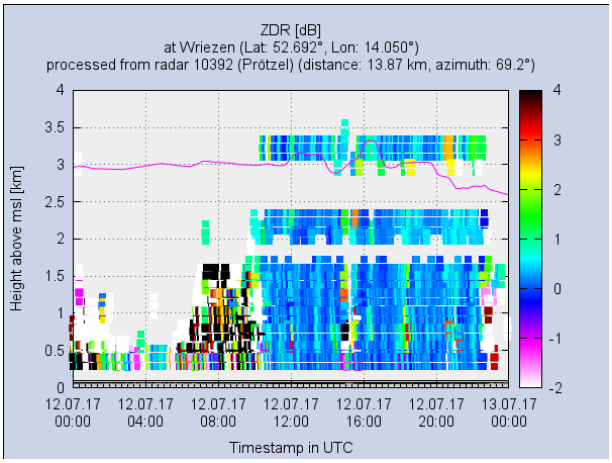

Figure 9: Time-height plot of ZDR 12 July 2017 for the Wriezen reference bin

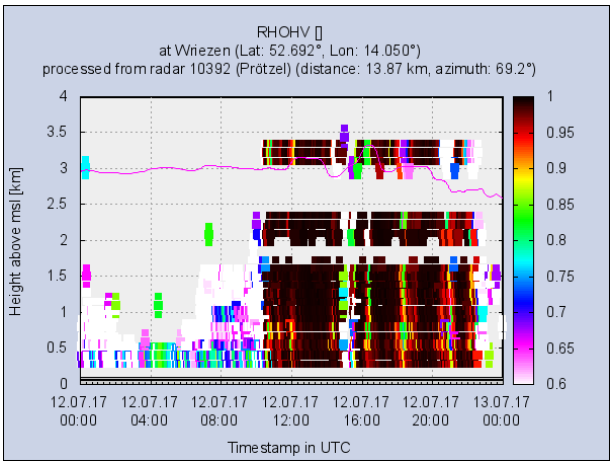

Figure 10: Time-height plot of RHOHV 12 July 2017 for the Wriezen reference bin

quality). From a meteorological point of view we are not able to provide information on the precipitation type over an area larger than 1 km^2. Based on the magnitude of the reflectivity factor, the precipitation is mainly of stratiform nature. However there are small scale convective pockets embedded in the stratiform precipitation where graupel is classified bye the HMC (Figure 11). The presence of graupel is indicated by observed lightning activity for this case. So a simple interpolation to fill the area using the surrounding information bears substantial uncertainty because of the non-homogenous precipitation field.

7. Summary

In this contribution we have investigated the influence of wind turbines on operational radar data, their quality and the subsequent radar products, namely a hydrometeor classification. In addition we have analyzed dedicated so called clutter target scans where the radar is dwelling on a TV tower (which is considered as a classic cutter target) and a wind turbine (WT) at the boundary of a wind farm. Those data show that the Doppler clutter filter cannot separate the WT signal from the meteorological signal.

There is large variability of Φ_{dp} in the presence of WTs. This is crucial, because the texture of Φ_{dp} is an important parameter in DWD's operational quality control of

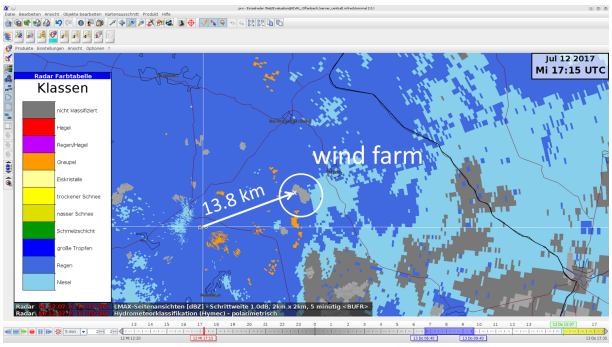

Figure 11: HMC result in the Wriezen area as seen in the forecaster's meteorological visualization and analysis system Ninjo.

radar data. This presumably leads to the thresholding of the Wriezen wind farm area. From a data quality point of view this is encouraging, because we are able to detect the wind farm influence in radar in this case. However, in this particular case a simple interpolation to fill the gap seems questionable because of the heterogeneity of the precipitation field. Here, the heterogeneity is given is by convective pockets embedded in a stratiform rain event. Those convective areas include the HM class graupel. That there was actually graupel present is indicated by the observed lightning activity.

Time-height plots of the operational HMC for a given range shows that there are a substantial number of range bins at the the lowest elevation which are attributed to drizzle / rain prior to the actual precipitation. There is also a significant number of range bins that cannot be assigned to any HM class. This is due to the fact that radar moments influenced by WT cannot be effectively filtered by quality control. Those range bins are not only confined to the lowest elevation. They are found up to a height of 1.5 km, which indicates that WTs become visible at higher elevations through side lobes. That this is can be attributed to WTs is indicated by the fact that the number of unclassified HM range bins is significantly smaller over the Manschnow site which serves as a reference site where no WTs are present.

References

Al-Sakka, H., A.-A. Boumahmoud, B. Fradon, S. J. Frasier, and P. Tabary: 2013, A new fuzzy logic hydrometeor classification scheme applied to the french x-, c-, and s-band polarimetric radars. *J. Appl. Meteor. Climatol.*, **52**, 2328–2344.

Frech, M. and J. Seltmann: 2014, Effects of wind power plants in radar data. *8th Europ. Conf. On Radar in Meteor. and Hydrol., ERAD*.

Frech, M. and J. Steinert: 2015, Polarimetric radar observations during an orographic rain event. *Hydrology and Earth System Sciences*, **19**, 1141–1152.

Keränen, R., L. C. Alku, A. Pettazzi, and S. Salson: 2014, Weather radar and abundant wind farming - impacts on data quality and mitigation by doppler dual-polarization. *European Radar Conference ERAD, Garmisch-Partenkirchen*, ERAD, 18pp.

Norin, L.: 2015, A quantitative analysis of the impact of wind turbines on operational doppler weather radar data. *Atmos. Meas. Tech.*, **8**, 593–609.

Park, H., A. V. Ryzhkov, D. S. Zrnić, and K.-E. Kim: 2009, The hydrometeor classification algorithm for the polarimetric WSR-88D: Description and application to an MCS. *Weather & Forecasting*, **24**, 730–748.

Werner, M. and J. Steinert: 2012, New quality assurance algorithms for the DWD polarimetric C-band weather radar network. *7th Europ. Conf. On Radar in Meteor. and Hydrol.*, number NET403.